



Emergence of a Novel *Salmonella enterica* Serotype Reading Clonal Group Is Linked to Its Expansion in Commercial Turkey Production, Resulting in Unanticipated Human Illness in North America

Elizabeth A. Miller,^a Ehud Elnekave,^b Cristian Flores-Figueroa,^c Abigail Johnson,^a Ashley Kearney,^d Jeannette Munoz-Aguayo,^c Kaitlin A. Tagg,^e Lorelee Tschetter,^d Bonnie P. Weber,^a Celine A. Nadon,^d Dave Boxrud,^f Randall S. Singer,^a Jason P. Folster,^g Timothy J. Johnson^{a,c}

^aDepartment of Veterinary and Biomedical Sciences, College of Veterinary Medicine, University of Minnesota, Saint Paul, Minnesota, USA

^bDepartment of Veterinary Population Medicine, College of Veterinary Medicine, University of Minnesota, Saint Paul, Minnesota, USA

^cMid-Central Research and Outreach Center, University of Minnesota, Willmar, Minnesota, USA

^dPublic Health Agency of Canada, National Microbiology Laboratory, Winnipeg, Canada

^eWDS, Inc., Atlanta, Georgia, USA

^fMinnesota Department of Health, Saint Paul, Minnesota, USA

^gDivision of Foodborne, Waterborne, and Environmental Diseases, Centers for Disease Control and Prevention, Atlanta, Georgia, USA

ABSTRACT Two separate human outbreaks of *Salmonella enterica* serotype Reading occurred between 2017 and 2019 in the United States and Canada, and both outbreaks were linked to the consumption of raw turkey products. In this study, a comprehensive genomic investigation was conducted to reconstruct the evolutionary history of *S. Reading* from turkeys and to determine the genomic context of outbreaks involving this infrequently isolated *Salmonella* serotype. A total of 988 isolates of U.S. origin were examined using whole-genome-based approaches, including current and historical isolates from humans, meat, and live food animals. Broadly, isolates clustered into three major clades, with one apparently highly adapted turkey clade. Within the turkey clade, isolates clustered into three subclades, including an “emergent” clade that contained only isolates dated 2016 or later, with many of the isolates from these outbreaks. Genomic differences were identified between emergent and other turkey subclades, suggesting that the apparent success of currently circulating subclades is, in part, attributable to plasmid acquisitions conferring antimicrobial resistance, gain of phage-like sequences with cargo virulence factors, and mutations in systems that may be involved in beta-glucuronidase activity and resistance towards colicins. U.S. and Canadian outbreak isolates were found interspersed throughout the emergent subclade and the other circulating subclade. The emergence of a novel *S. Reading* turkey subclade, coinciding temporally with expansion in commercial turkey production and with U.S. and Canadian human outbreaks, indicates that emergent strains with higher potential for niche success were likely vertically transferred and rapidly disseminated from a common source.

IMPORTANCE Increasingly, outbreak investigations involving foodborne pathogens are difficult due to the interconnectedness of food animal production and distribution, and homogeneous nature of industry integration, necessitating high-resolution genomic investigations to determine their basis. Fortunately, surveillance and whole-genome sequencing, combined with the public availability of these data, enable comprehensive queries to determine underlying causes of such outbreaks. Utilizing this pipeline, it was determined that a novel clone of *Salmonella Reading* has emerged that coincided with increased abundance in raw turkey products and two

Citation Miller EA, Elnekave E, Flores-Figueroa C, Johnson A, Kearney A, Munoz-Aguayo J, Tagg KA, Tschetter L, Weber BP, Nadon CA, Boxrud D, Singer RS, Folster JP, Johnson TJ. 2020. Emergence of a novel *Salmonella enterica* serotype Reading clonal group is linked to its expansion in commercial turkey production, resulting in unanticipated human illness in North America. *mSphere* 5:e00056-20. <https://doi.org/10.1128/mSphere.00056-20>.

Editor Brandi M. Limbago, U.S. Centers for Disease Control and Prevention

Copyright © 2020 Miller et al. This is an open-access article distributed under the terms of the [Creative Commons Attribution 4.0 International license](https://creativecommons.org/licenses/by/4.0/).

Address correspondence to Timothy J. Johnson, tjj@umn.edu.

 Phylogenomic analyses describe key mutational events leading to the emergence of a novel clonal group of *Salmonella Reading* linked to ground turkey outbreaks in the US and Canada @MinnMicroProf @crumpetliz

Received 17 January 2020

Accepted 26 March 2020

Published 15 April 2020

outbreaks of human illness in North America. The rapid dissemination of this highly adapted and conserved clone indicates that it was likely obtained from a common source and rapidly disseminated across turkey production. Key genomic changes may have contributed to its apparent continued success in commercial turkeys and ability to cause illness in humans.

KEYWORDS *Salmonella*, clone, genomic, human, outbreak, poultry, turkey

Salmonella enterica subsp. *enterica* derived from poultry meat serves as a primary cause of salmonellosis infections in humans within the United States and worldwide (1, 2). Among the more than 2,500 serotypes that have been identified thus far, only a handful of them consistently top the list as those causing the majority of cases of human illness. Estimates on human salmonellosis cases from poultry in the United States vary, depending on the method used, from 10 to 29%, and the estimate for cases specifically from turkeys numbers 5.5% (3, 4).

S. Reading is a serotype of *S. enterica* subsp. *enterica* first identified in 1916 from a water supply in Reading, England (5), and subsequently identified in various animal hosts, including poultry (6–10). Human outbreaks due to *S. Reading* historically have been relatively infrequent. In 1956 to 1957, an outbreak involving *S. Reading* occurred in the United States, sickening 325 people across multiple states (11). In 2008, 30 persons were involved in an outbreak linked to iceberg lettuce in Finland (12). In 2014 to 2015, an outbreak of unknown origin was described, with 31 confirmed cases in Canada involving persons of Mediterranean descent (13).

Commercial turkey production is commonly identified as a primary reservoir of *S. Reading* (2, 14–17). Given its low isolation frequency, relatively little is known about the biology of *S. Reading* compared with other serotypes. With that said, *S. Reading* has been shown to have enhanced ability to form biofilms under stress conditions (18) and has been isolated from produce (19). Multidrug resistance phenotypes, including resistance towards third-generation cephalosporins, also appear to be common in *S. Reading* strains, including those in dairy cows and beef feedlot cattle (20–22).

Two separate, large outbreaks of *S. Reading* were recently reported in North America. In the United States, the Centers for Disease Control and Prevention declared an outbreak from November 2017 through March 2019 (23), although human cases of salmonellosis due to *S. Reading* have continued (as of January 2020). The outbreak was linked to live turkeys and raw turkey products, but no single source product or company was attributed to the entire outbreak. This outbreak resulted in 358 illnesses, 133 hospitalizations, and 1 death across 42 states. In Canada, a separate multiprovince outbreak was declared in October 2018 by the Public Health Agency of Canada, with a final report in February 2020 of 130 identified cases (24).

Given the widespread nature of these recent North American *S. Reading* outbreaks, there is a pressing need to better understand the ecology and evolution of this foodborne pathogen within suspected animal reservoirs. As such, the purpose of this study was to perform a comprehensive genomic investigation to reconstruct the evolutionary history of *S. Reading* and to determine whether underlying genomic changes within *S. Reading* correlated with outbreaks involving this rarely isolated *Salmonella* serotype.

RESULTS

***S. Reading* isolates cluster phylogenetically by host source.** Using assembled sequences ($n = 988$) from human illness, meat products, live animals, and environmental sources, isolates were first assigned to seven-gene multilocus sequence types (MLSTs) using the scheme from the PubMLST website (<https://pubmlst.org>) (25). Based on this scheme, six sequence types (STs) were identified with three dominating: one containing primarily turkey-source and human-source isolates (ST412; 83.5% of isolates), one containing primarily swine/bovine-source and human-source isolates (ST1628; 10.1% of isolates), and one containing primarily human-source isolates (ST93;

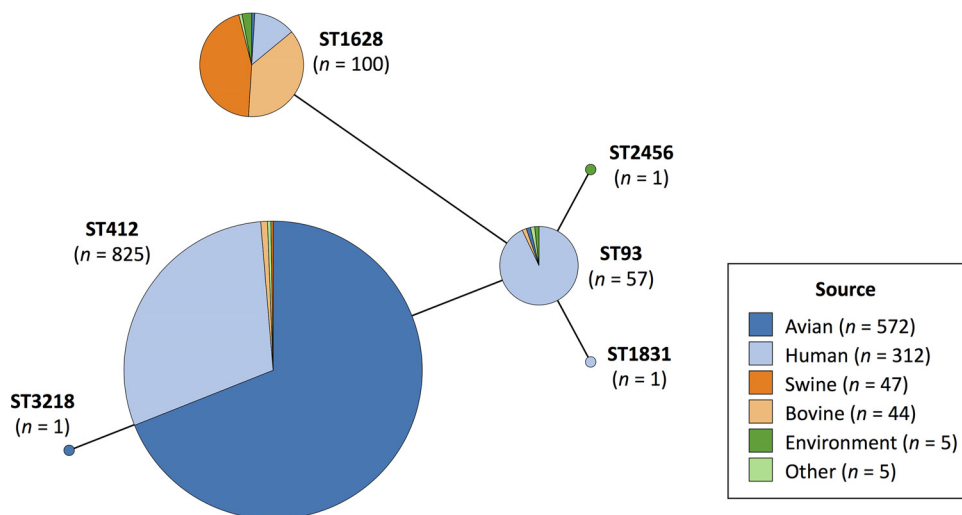


FIG 1 Minimum spanning tree of STs using the Achtman seven-gene MLST scheme for 985 *S. Reading* isolates. Three isolates (swine-, chicken-, and human-source isolates) are not included because their STs could not be determined. The tree is colored based on the isolate host source.

5.8% of isolates) (Fig. 1). Animal host source was strongly correlated with ST, with 99.6% (564/566) of total turkey-source isolates belonging to ST412 and 93.8% (45/48) and 84.1% (37/44) of swine-source and bovine-source isolates, respectively, belonging to ST1628. To rule out temporal bias in the clustering of same host-source isolates by ST, isolates were also characterized based on year of isolation using the same ST scheme (see Fig. S1 posted at <https://doi.org/10.6084/m9.figshare.11966550>). This demonstrated evenness with regard to isolation date across the major STs.

Core genome MLST (cgMLST) profiles based upon 3,002 loci were then identified for all isolates, allowing for up to either two allelic differences (see Fig. S2A posted at the above URL) or five allelic differences (see Fig. S2B posted at the above URL). In all analyses, there was clear and consistent separation based upon animal host source, separating isolates into three major groups.

To gain further resolution, a whole-genome core single nucleotide polymorphism (SNP)-based phylogenetic tree was constructed for all isolates (Fig. 2; see Fig. S3 posted at the above URL for a greater resolution tree including all bootstrap values). The resulting tree contained 11,086 core SNPs and resolved isolates into three primary clades (designated clades 1 to 3), corresponding to MLST and cgMLST results. Clade 1 ($n = 828$) was comprised mainly of turkey-source and human-source isolates, and all but one turkey-source isolate fell within this clade. Clade 2 ($n = 59$) was primarily human-source isolates. Clade 3 ($n = 101$) contained mainly swine-source and bovine-source isolates, with 95.8% (46/48) and 84.1% (37/44) of total swine-source and bovine-source isolates falling within this clade, respectively. Average core SNP distances were investigated between clades (see Table S1 posted at <https://doi.org/10.6084/m9.figshare.11966550>), revealing that clades 1 and 2 were more similar to one another (mean core SNP difference, $1,638.72 \pm 8.49$) than clades 1 and 3 ($8,165.04 \pm 10.91$) or clades 2 and 3 ($9,246.30 \pm 12.72$). Additionally, mean SNP differences for isolates within clade 1 (7.72 ± 5.61) were lower than those within clade 2 (59.23 ± 44.10) or clade 3 (32.87 ± 16.84). To confirm that these results were not due to different sample sizes between clades, average core SNP distances were recalculated on a random subsample of each clade (see Table S1 posted at the above URL).

Genome sizes also varied between the three clades, with clade 2 containing the smallest genomes (median, 4.53 ± 0.095 Mb), which were on average 114.50 kb smaller than clade 1 genomes (median, 4.64 ± 0.050 Mb) and 396.25 kb smaller than clade 3 genomes (median, 4.92 ± 0.10 Mb) (see Fig. S4 posted at the above URL).

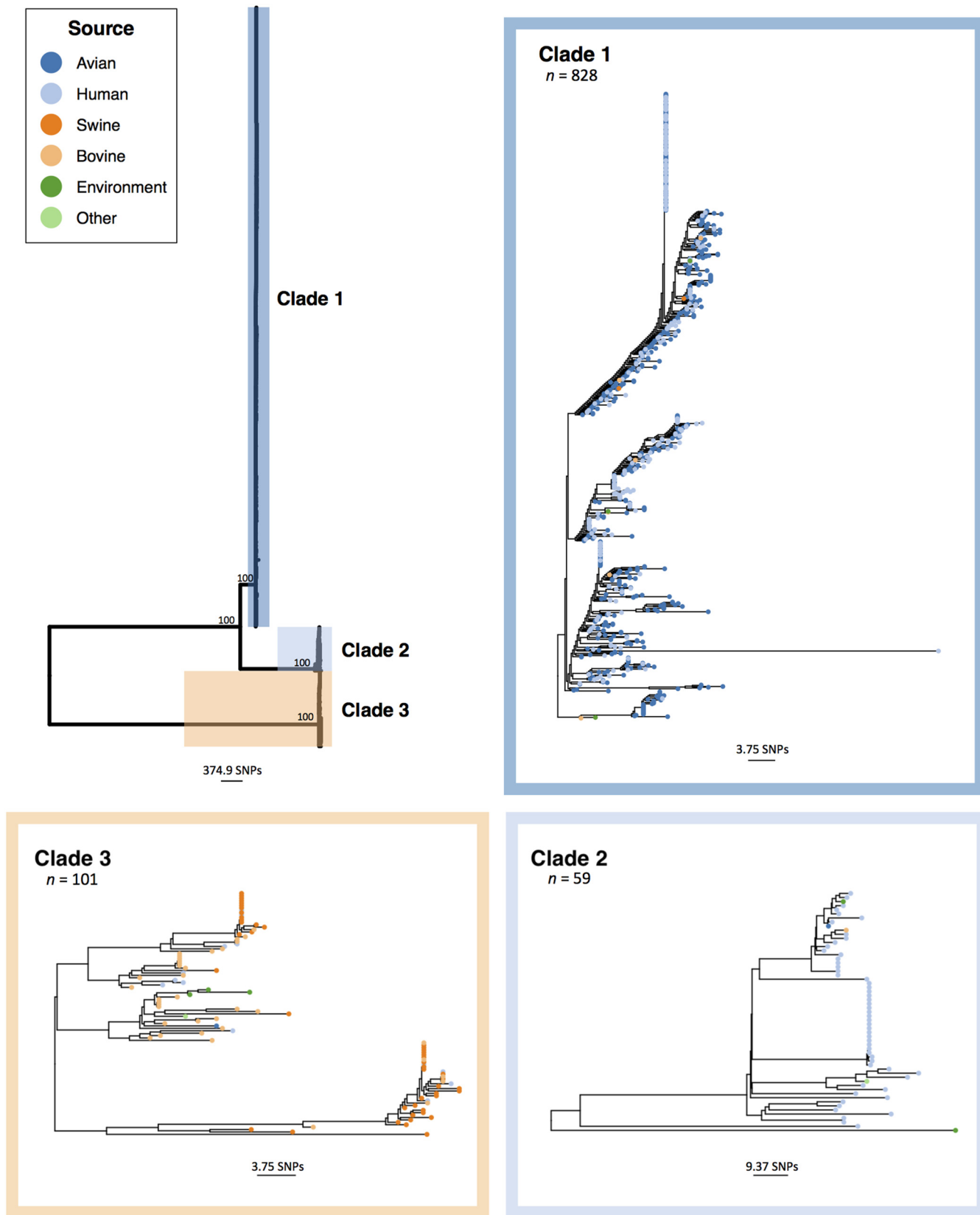


FIG 2 Midpoint-rooted phylogenetic tree of *S. Reading* isolates ($n = 988$) based on core SNPs in nonrecombinant genome regions. All isolates fell into one of three clades: clade 1 (dark blue; primarily turkey- and human-source isolates), clade 2 (light blue; primarily human-source isolates), and clade 3 (orange; primarily swine- and bovine-source isolates). Bootstrap values are shown at the branches differentiating between clades. To allow for a finer-scale view of clade topology, insets show each clade independently (note the difference in scale bars). The color of the circles at the tips indicates the isolate host source.

A pan-genome approach was then used to investigate specific genomic differences between isolates from clades 1 and 3, representing the majority of isolates from turkey and swine/bovine sources, respectively. A total of 11,366 gene clusters were identified across all 988 isolates, with 3,246 (28.6%) present in 100% of isolates (i.e., the “core” genes). Using a cutoff requirement of 100% prevalence versus 0% prevalence in the two populations, a total of 225 gene clusters were identified as unique to clade 1, and 180 gene clusters were unique to clade 3 (see Dataset S1 posted at <https://doi.org/10.6084/m9.figshare.11966550>). Clade 1 isolates had 15 unique fimbrial system component genes clustered across three systems, including *yadKLMNV*, *yehABCD*, and a novel K88-like fimbrial system, all of which were inserted in separate genomic locations with genes for each respective system clustered together. Clade 1 isolates also uniquely possessed *prgHIK* and *orgAB*, which are components of the *Salmonella* pathogenicity-associated island SPI-1 (26), genes annotated as cytolethal distending toxin *cdtAB*, and several prophage-like elements. Conversely, clade 3 isolates possessed a number of unique fimbria-like and prophage-like elements compared to those from clade 1. Also unique to clade 3 isolates were systems predicted to be involved in type I restriction modification, phosphotransferase activity, and CRISPR/Cas activity.

A recently emerged clade exists among turkey-source *S. Reading* isolates. The turkey-source isolates from clade 1 were then examined alone to gain further insight towards their evolution over time. All of these isolates ($n = 565$), except one, belonged to ST412 and were examined at higher resolution using a core SNP-based phylogenetic tree (Fig. 3). The phylogenetic tree contained 1,093 informative variant sites, and from this, three major subclades were designated based upon tree clustering and dates of isolation. The “historical” subclade (orange subclade in Fig. 3; $n = 65$) contained isolates dating 1999 to 2008. The “contemporary” subclade (purple subclade in Fig. 3; $n = 201$) contained isolates dating 2009 to 2019, with the majority from 2009 to 2016. Finally, the “emergent” subclade (blue subclade in Fig. 3; $n = 295$) contained isolates all dating 2017 to 2019, except for one from 2016. Four isolates were not assigned to a specific subclade due to their intermediate location between the contemporary and emergent subclades (black “basal” subclade in Fig. 3).

The same three-subclade structure was also observed in a minimum spanning tree from cgMLST data allowing for up to two allelic differences (Fig. 4), where isolates clearly separated by subclade designation (historical, contemporary, and emergent) and 57.6% of all isolates in the emergent subclade were of the same cgMLST profile. A phylogenetic tree constructed from core genome SNPs and a dendrogram based on hierarchical clustering of all pan-genome genes also showed isolates clustered into the same three subclades (see Fig. S5 posted at the above URL).

Based upon average core SNP distances (Table 1), the emergent and contemporary subclades were more similar to each other (mean core SNP difference, 14.35 ± 3.08) than emergent versus historical subclade (39.95 ± 11.38) or contemporary versus historical subclades (42.58 ± 11.59). Within subclades, emergent subclade isolates were more similar to each other (4.67 ± 2.13) than were isolates from the contemporary (10.92 ± 3.88) or historical (33.63 ± 18.37) subclade.

Small plasmids and associated resistance genes define differences between turkey-source clades. All clade 1 turkey-source isolates were examined for their possession of genes and mutations known to confer antimicrobial resistance and plasmid replicons known among Gram-negative bacteria (Fig. 5). When overlaid on the SNP-based phylogenetic tree, several patterns emerged. First, nearly all isolates contained a T57S mutation in *parC* and the ColpVC plasmid replicon. An IncQ1 plasmid replicon was found in 20% (41/201) and 33% (98/295) of isolates belonging to the contemporary and emergent subclades, respectively. The possession of this plasmid replicon was significantly associated with possession of *sul2*, *tet(A)*, *strA* [*aph(3'')-Ib*], and *strB* [*aph(6)-Id*] genes conferring the classical SSuT phenotype (see Table S2 posted at <https://doi.org/10.6084/m9.figshare.11966550>; all pairwise Fisher’s exact test Benjamini-Hochberg (BH)-adjusted P values < 0.05). Possession of these traits were

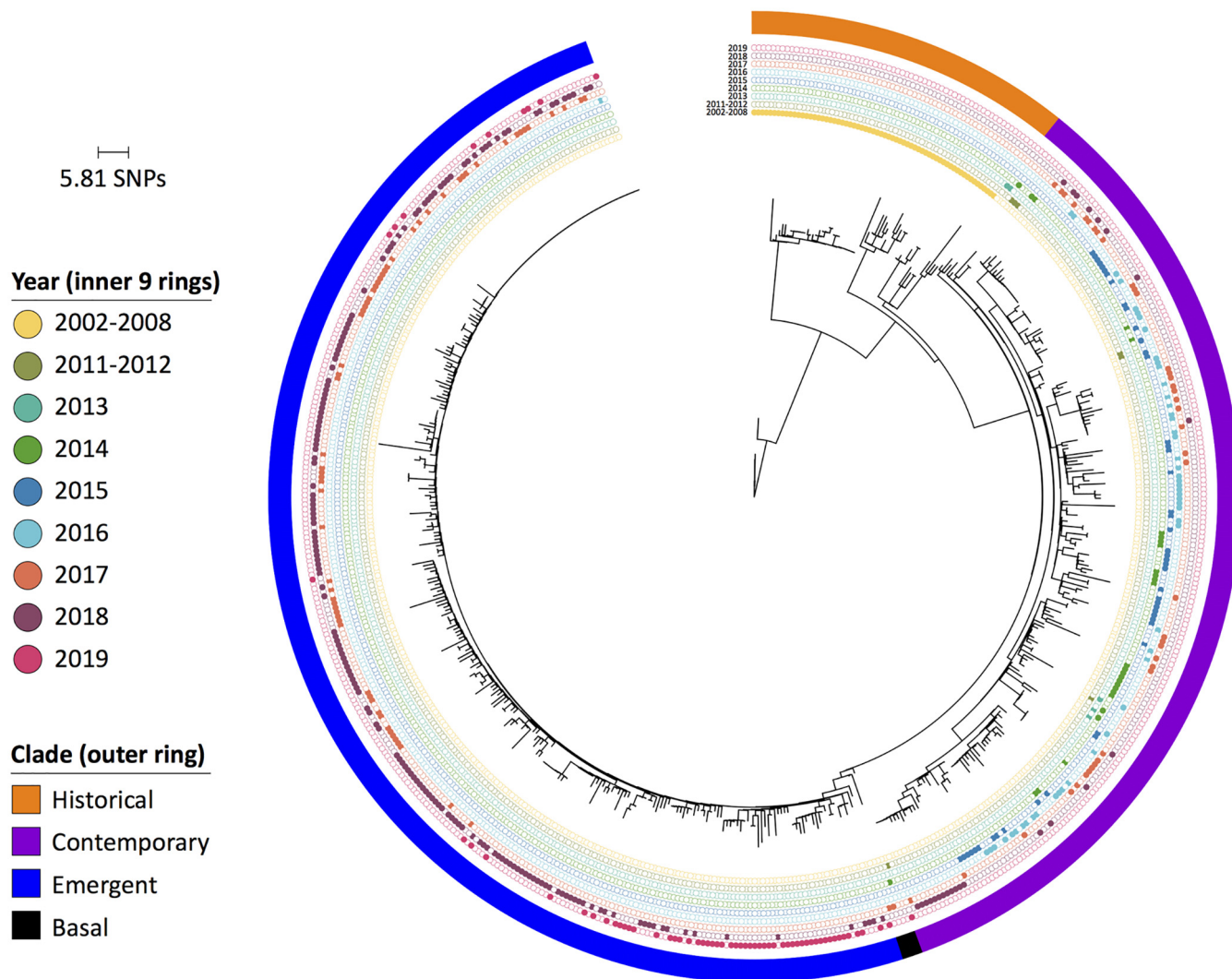


FIG 3 Phylogenetic tree of turkey-source *S. Reading* isolates ($n = 565$) based on core SNPs in nonrecombinant genome regions. The majority of isolates were grouped based on clustering and isolation year into three subclades shown in the outer ring. The inner nine rings show years of isolation, with filled circles depicting the year for an individual isolate. The tree is rooted with an isolate collected in 2002 (SRR1195634).

found throughout the emergent subclade, with some evidence of trait loss scattered infrequently. In contrast, isolates possessing these traits in the contemporary subclade were found clustered in one half of the subclade and were absent from the other half.

Isolates belonging to the emergent subclade also frequently possessed co-occurring ColRNAI-like and Col440II-like plasmid replicons, present in 61% (181/295) and 65% (191/295) of isolates within this subclade, respectively. Isolates in the emergent subclade were more than 20 times more likely to possess both replicons compared to isolates in the historical and contemporary subclades (Fisher's exact test: odds ratio = 0.022, P value < 0.05). Possession of these replicons was also significantly associated with possession of the beta-lactam resistance gene, *bla*_{TEM-1C} (see Table S2 posted at the URL mentioned above; all pairwise Fisher's exact test BH-adjusted P values < 0.05).

Complete sequences of these highly conserved plasmids belonging to IncQ1 and Col440II/ColRNAI-like replicon types were identified and annotated from a representative turkey-source isolate (Fig. 6). The IncQ1 replicon and *sul2-strAB-tetAR* genes were colocalized within a 10,867-bp mobilizable plasmid containing *mobAC*. The Col440II- and ColRNAI-like replicons were found on a 10,384-bp mobilizable plasmid containing *mobAD* and *bla*_{TEM-1C} adjacent to a Tn2 transposon.

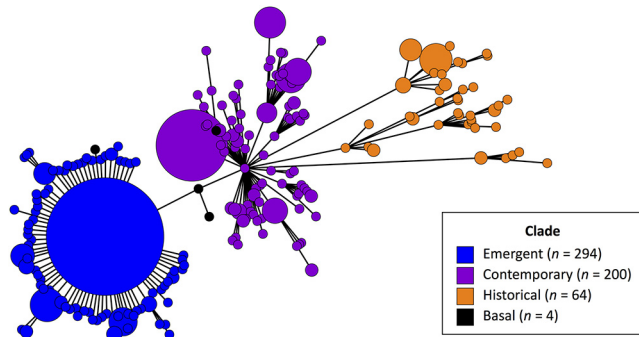


FIG 4 Minimum spanning tree of turkey-source isolates ($n = 562$) using the core genome sequence typing (cgMLST) scheme allowing for up to two allelic differences. Three isolates are not included because their cgMLST profiles could not be determined. Tree colors are based on core SNP-based phylogenetic tree subclade designations (see Fig. 3). Four isolates not assigned to a specific subclade are classified as basal to the emergent subclade (black color).

To better understand the emergence of this Col440II/ColRNAI plasmid variant, all surveillance data from the European Nucleotide Archive (ENA) and NCBI Short Read Archive (SRA) databases (until December 2016) were searched for a 282-bp region of the Col440II-like replicon (see Fig. S6 posted at <https://doi.org/10.6084/m9.figshare.11966550>). The first available sequence of the replicon was identified in *S. enterica* in 2000, but it did not carry *bla*_{TEM-1C}. The first detection of this plasmid replicon carrying *bla*_{TEM-1C} was from a turkey-source *S. Hadar* isolate in 2007, and the appearance of this plasmid replicon in *S. Hadar* coincided with subsequent foodborne outbreaks implicating live poultry or poultry products (27, 28), with isolates from those outbreaks containing highly similar plasmids (nucleotide blast of draft assemblies; data not shown). The first detection of this plasmid replicon, including *bla*_{TEM-1C} in *S. Reading* was from a turkey-source isolate in 2014.

Pan-genome-wide association analysis suggests that clusters of bacteriophage-associated genes and other elements were gained and lost over time. Comparison of average genome sizes between subclades showed an increase in size from the historical subclade (median, 4.58 ± 0.051 Mb) to the contemporary subclade (median, 4.66 ± 0.046 Mb) and a subsequent decrease in size to the emergent subclade (median,

TABLE 1 Comparison of mean core SNP differences between unique core SNP profiles in the same and different turkey-only phylogenetic subclades

Subclade comparison	SNP difference		
	Mean \pm SD	Minimum	Maximum
All profiles ^a			
Overall	16.74 \pm 14.04	1	78
Emergent	4.67 \pm 2.13	1	18
Contemporary	10.92 \pm 3.88	1	23
Historical	33.63 \pm 18.37	1	73
Emergent vs contemporary	14.35 \pm 3.08	6	29
Emergent vs historical	39.95 \pm 11.38	23	78
Contemporary vs historical	42.58 \pm 11.59	21	77
Random profile subset ^b			
Overall	27.18 \pm 17.51	1	76
Emergent	5.27 \pm 1.95	1	12
Contemporary	10.89 \pm 4.13	1	22
Historical	33.63 \pm 18.37	1	73
Emergent vs contemporary	14.61 \pm 3.19	8	24
Emergent vs historical	40.18 \pm 11.41	24	74
Contemporary vs historical	41.61 \pm 11.60	22	76

^aThe numbers of unique core SNP profiles were as follows: $n = 44$ for the historical subclade, $n = 151$ for the contemporary subclade, and $n = 200$ for the emergent subclade.

^bFor the random profile subset, there were 44 unique core SNP profiles from each subclade.

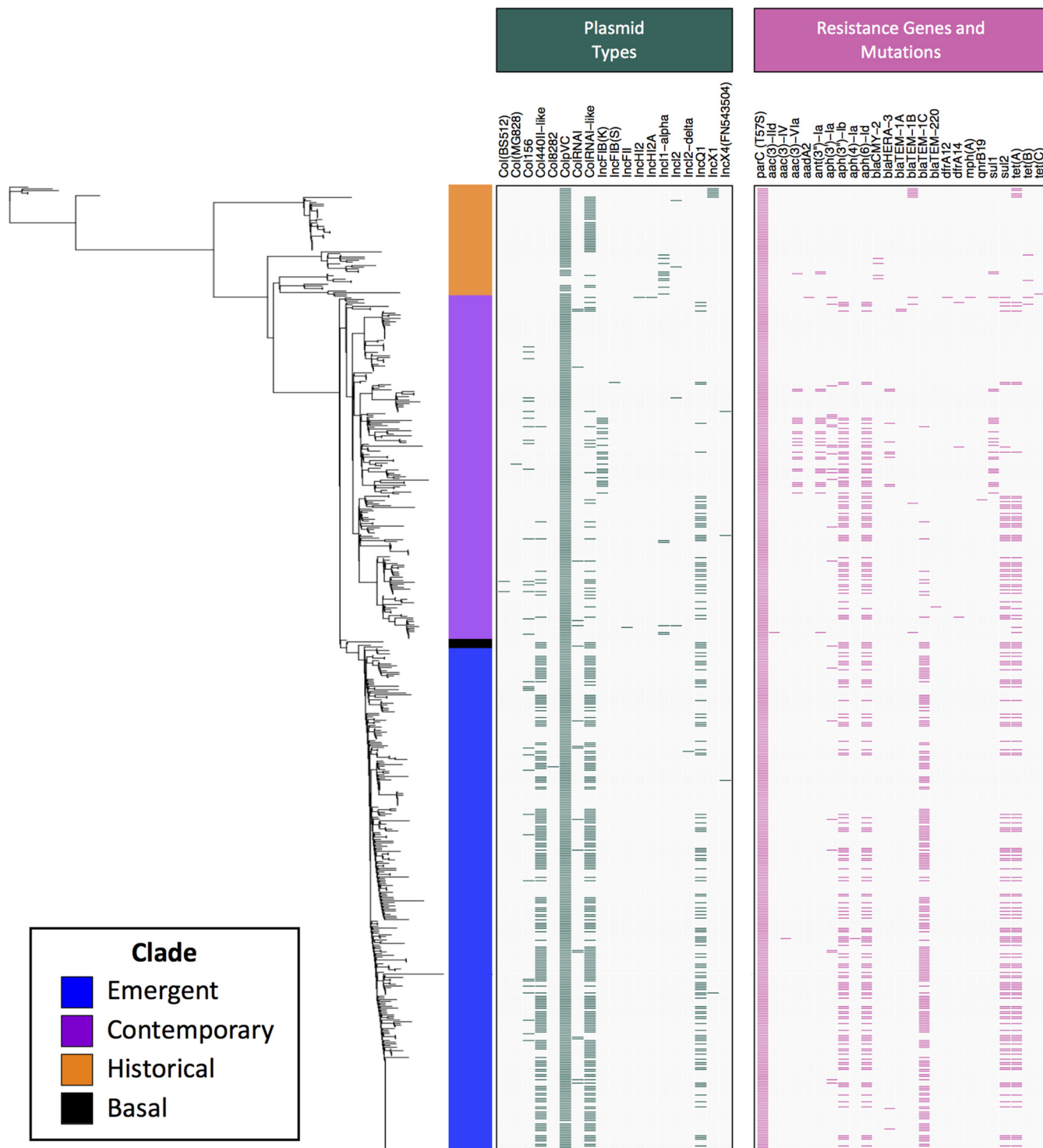


FIG 5 Heatmap displaying the presence of plasmid replicons (dark green) and genes and mutations conferring antimicrobial resistance (pink) across clade 1 turkey-source isolates.

4.63 ± 0.016 Mb) (see Fig. S4 posted at the above URL). A pan-genome analysis was used to identify specific genes contributing to this shift in genome size between subclades. A total of 6,747 gene clusters were produced, of which 3,763 (56%) were core genes. Of the 2,984 accessory genes, the majority (79%) were found in less than 15% of isolates (see Fig. S7 posted at the above URL).

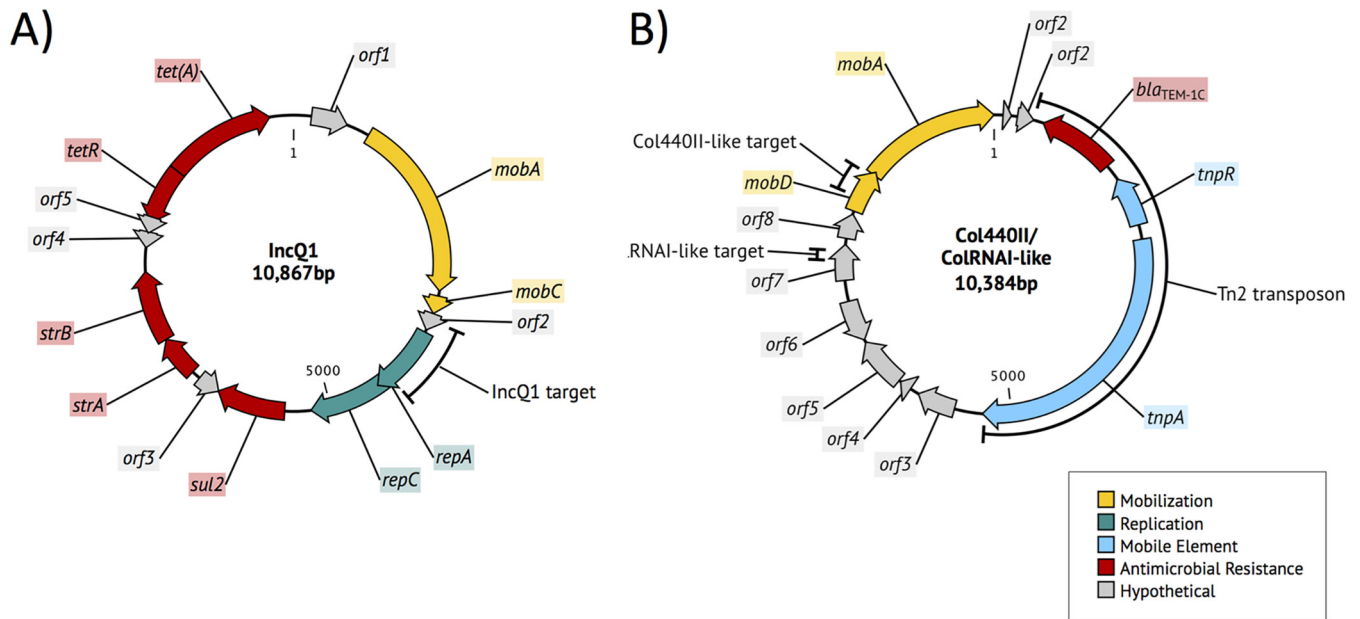


FIG 6 Circular genetic maps of IncQ1 (A) and Col440II/ColRNAI-like (B) plasmids. Arrows indicate predicted genes and the direction of transcription and are colored to indicate predicted functional category.

Pan-genome-wide association analysis identified 134 genes with significantly differential prevalence between the historical, contemporary, and emergent subclades (Fig. 7; see Dataset S2 posted at <https://doi.org/10.6084/m9.figshare.11966550>). A large collection of genes primarily encoding bacteriophage-related proteins was absent from the majority of both historical and emergent isolates (<2.5%) but was found in most contemporary isolates (93%) (phage region A in Fig. 7). Based on annotations of the representative genome assembly, SRR2407706, all of these genes were clustered in a single region of the *S. Reading* genome (Fig. 8; see Fig. S8 posted at the above URL), and the majority were homologous to genes from bacteriophages HP1 and HP2. Two separate collections of bacteriophage-related genes were absent from all historical subclade isolates, but present in more than 99% of contemporary and emergent subclade isolates (phage regions B and C in Fig. 7). Both gene clusters could be mapped to separate regions of the *S. Reading* genome (Fig. 8; see Fig. S8 posted at the above URL), with phage region B genes homologous to genes primarily found in lambda phages GIFSY-1 and GIFSY-2 and phage region C genes homologous to a range of *Enterobacterium*-specific phages. Of particular note, phage region B included the bacterial virulence-associated gene *sopE* encoding a type III secretion protein effector, which was surrounded by genes encoding phage tail and fiber proteins and an ISL3 family transposase.

Of the 13 genes significantly associated with the emergent subclade, 10 were identified as part of the Col440II/RNAI-like plasmid. These 10 genes included genes encoding TEM-1C beta-lactamase, Tn2 transposase and resolvase, mobilization proteins A and D, and five hypothetical proteins. The Col440II-like replicon was significantly more common in isolates from the emergent subclade than in isolates from either the historical or contemporary subclades (all pairwise Fisher's exact test BH-adjusted *P* values < 0.05) (see Tables S3 and S4 posted at the above URL). Additionally, *cirA*, which encodes a colicin Ia/b receptor, was identified intact in 93.5% of isolates in the contemporary and historical subclades but was disrupted in the majority (96.9%) of isolates from the emergent subclade due to a frameshift insertion of cytosine at position 680. In some of the contemporary subclade isolates, amino acids 47 to 69 of *cirA* were truncated, representing a distinct disruption of CirA compared to the emergent isolates. Similarly, a full-length *uidA*-like gene, which is predicted to encode a

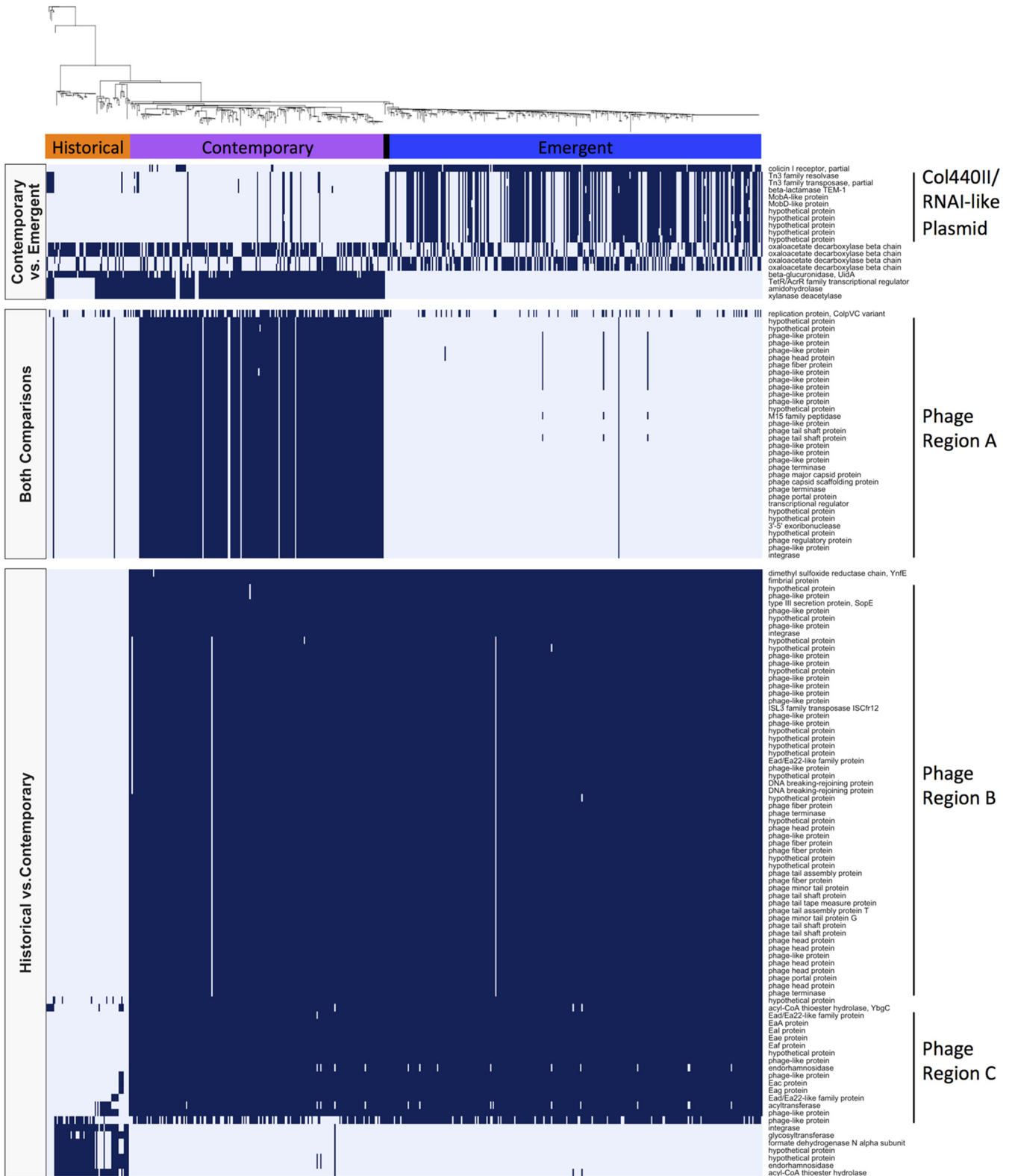


FIG 7 Heatmap displaying the presence (dark blue) and absence (light blue) of genes with significant associations to the historical, contemporary, and/or emergent subclades. Left-hand side labels group genes based on the comparison they were identified in: historical versus contemporary, contemporary versus emergent, or both comparisons. Right-hand side labels denote genes that clustered into a single region of the *S.* Reading genome.

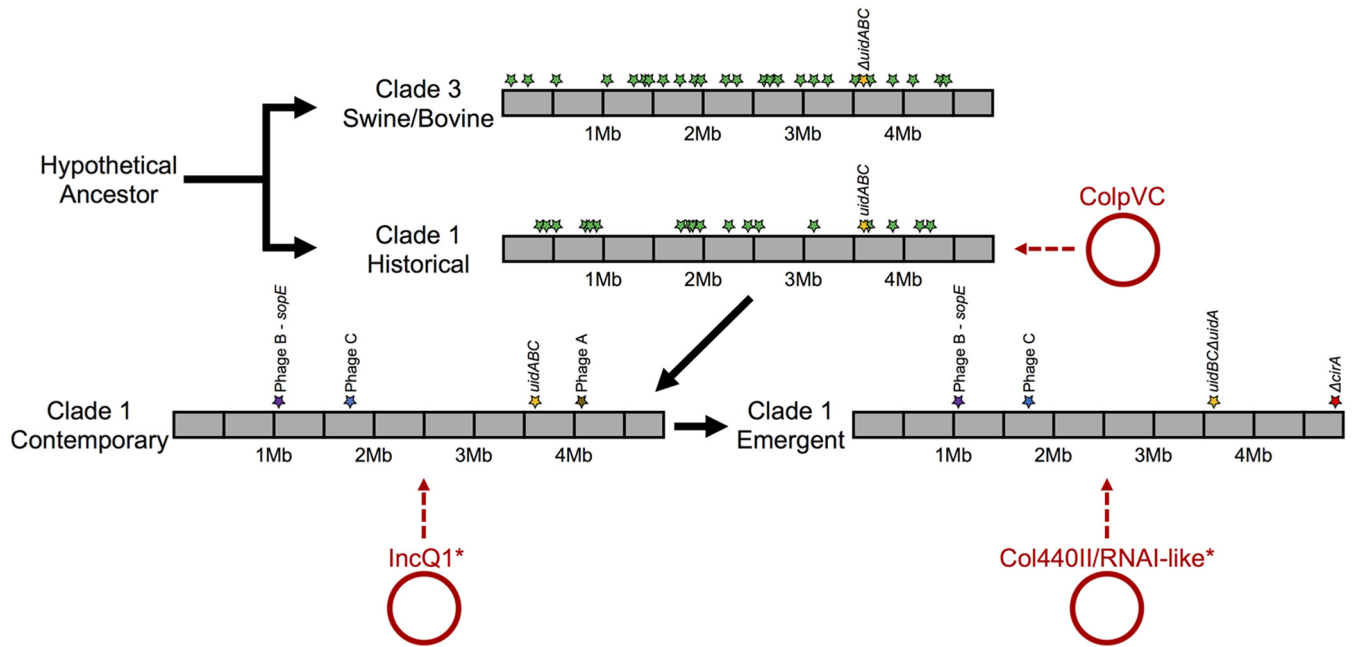


FIG 8 Genetic changes leading from the hypothetical ancestor of *S. Reading* through the current emergent turkey-source clonal group. Green stars indicate unique genomic islands differing between clades 1 and 3. Purple, blue, and brown stars indicate insertions within clade 1 contemporary and emergent isolates relative to historical subclade isolates. The gold star indicates insertion of *uidABC*-like region in clade 1 isolates, where the *uidA*-like gene was subsequently truncated in emergent subclade isolates. The red star indicates a truncation of the *cirA* gene in clade 1 emergent subclade isolates. Plasmid acquisitions are denoted by circles and dashed arrows. Note that *IncQ1* and *Col440II/RNAI-like* plasmids are found in some other clades but become dominant in the denoted subclades.

beta-glucuronidase enzyme, was present in 89.8% of contemporary and historical subclade isolates but truncated in all emergent subclade isolates. Interestingly, *uidABC* was also found to be absent from clade 3 isolates in unique fashion compared to clade 1 emergent subclade isolates.

Time-scaled phylogenetic analysis. A time-scaled phylogeny of turkey-source sequences ($n = 398$ after removal of duplicated sequences) was reconstructed using a general time reversible (GTR) nucleotide substitution model, an uncorrelated lognormal relaxed molecular clock, and a constant growth coalescent model (see Fig. S9 at <https://doi.org/10.6084/m9.figshare.11966550>). The model predicted an evolutionary rate of 4.14×10^{-7} substitutions/site/year (95% higher posterior density [HPD₉₅] = 3.60×10^{-7} to 4.77×10^{-7}) and time to most recent common ancestor (TMRCA) for clade 1 was dated to 1984 (1975 to 1992). The branching of the contemporary and emergent subclades was dated to 1997 (1994 to 1997) with the emergent subclade arising in 2015 (2014 to 2016).

North American *S. Reading* outbreak isolates cluster with both contemporary and emergent subclade turkey-source isolates. To investigate the two recent North American *S. Reading* outbreaks in the context of turkey-source *S. Reading* strains, a core SNP-based phylogenetic tree was constructed for all clade 1 turkey-source isolates ($n = 565$) and human-source isolates identified as part of the 2017–2019 *S. Reading* outbreaks in the United States ($n = 139$) and Canada ($n = 111$) (see Fig. S10 posted at the above URL). Outbreak isolates from both countries were found clustered with turkey-source isolates from both the contemporary and emergent subclades. Specifically, for the U.S. outbreak isolates, 29.5% (41/139) of isolates clustered with the contemporary subclade and 69.1% (96/139) with the emergent subclade. For Canadian outbreak isolates, the distribution was more balanced between subclades, with 47.7% (53/111) clustering with the contemporary subclade and 52.3% (58/111) with the emergent subclade. A subset of both U.S. and Canadian outbreak isolates shared identical core SNP profiles with some turkey-source isolates. In particular, one prevalent

TABLE 2 Human cases of *S. Reading* compared with percentage of human-source isolates used in this study that cluster with turkey-source isolates^a

Year	No. of cases		% cases associated with the following subclade:	
	CDC	MNDH	Contemporary	Emergent
2008	46	3	ND	ND
2009	53	3	ND	ND
2010	33	1	ND	ND
2011	42	1	ND	ND
2012	58	3	0	0
2013	55	2	0	0
2014	104	4	82	0
2015	139	7	88	0
2016	221	7	59	2
2017	ND	13	44	29
2018	ND	21	23	63

^aHuman cases of *S. Reading* reported by the CDC and Minnesota Department of Health (MNDH), compared with percentage of human-source isolates used in this study that cluster with turkey-source contemporary or emergent subclade isolates. ND, no human case data available.

SNP profile was found in 96 isolates, including 56 turkey-source isolates, 28 U.S. outbreak isolates, and 12 Canadian outbreak isolates. Mining of CDC and Minnesota of Department of Health data suggests an increase in *S. Reading* starting in 2014 involving clade 1 contemporary subclade isolates. Increases in *S. Reading* cases were further amplified by clade 1 emergent subclade isolates starting in 2016, which increased substantially in relative proportion in 2017 and 2018 (Table 2).

DISCUSSION

Multiple outbreaks of *S. Reading* in North America prompted an investigation of the microevolution of this serotype, as human-associated outbreaks due to *S. Reading* are infrequently reported compared with other common serotypes. Very clear separation was observed between turkey-source and bovine/swine-source *S. Reading* isolates, accompanied by large whole-genome SNP differences and numerous genomic island differences. This clear separation without intermediate isolates between the two clades (clade 1 versus clade 3) suggests that current clades represent distinct lineages associated with turkey versus bovine/swine hosts. Within clade 1, a time-scaled phylogeny reconstruction demonstrated the diversification of subclade branches with estimated node ages that align with the current North American outbreaks. In addition, these analyses estimated an evolutionary rate of 4.14×10^{-7} substitutions/site/year, which corresponds to a change of two SNPs per year. The constant population growth selected here may reflect the early stage of this clonal group's spread. The data indicate two distinct expansions of *S. Reading*. First, the contemporary subclade began the expansion in 2014 with an increased number of human cases compared to previous years (Table 2). In 2017, the number of human cases again expanded with the surfacing of the emergent subclade, coinciding with multiple outbreaks declared in the United States and Canada.

Genetic diversity within clade 1 was lowest compared to all clades studied here, and genetic diversity within the clade 1 emergent subclade isolates was extremely low. This, combined with dates of isolation, points to the recent emergence of a new clonal group of *S. Reading*, which was estimated to emerge in 2015 (HPD₉₅, 2014 to 2016) based on the time-scaled phylogeny reconstruction. This emergence coincides with large outbreaks in North America linked to contaminated turkey products, prompting the question of why this clonal group and associated serotype have become more successful. The overall genetic differences between the turkey subclades were subtle yet may provide important clues highlighting the success of strains within the contemporary and emergent subclades. One distinguishing feature of the emergent strains, and contemporary subsets of the circulating subclade, was the presence of mobilizable IncQ1 and Col440II/ColRNAI-like small plasmids. Collectively, these plasmids encode

resistance towards ampicillin, streptomycin, sulfamethoxazole, and tetracycline. IncQ1 plasmids are broad-host-range, highly mobilizable plasmids capable of residing in a variety of Gram-negative bacterial species (29). Similar conformations of this plasmid conferring the same SSuT resistance profile have been identified in *Salmonella* Typhimurium in Italy (30). While the presence of these two plasmids appears to be a marker of evolution of the subclade, they apparently have been frequently lost by isolates in the emergent subclade. There was no association between isolate host source and apparent plasmid loss (i.e., human- versus turkey-source isolates), indicating that plasmid loss is not a function of selective pressure in a particular environment but instead a function of genetic gain followed by plasmid instability or dispensability.

There was an overall genome size gain between the historical to contemporary/emergent subclade isolates within clade 1. This was primarily due to acquisition of several phage-like elements within the chromosome. Acquisition of a lambda-like prophage-like element was accompanied by accessory carriage of *sopE* into the contemporary and emergent subclades (Fig. 8). All clade 1 turkey strains carried the canonical version of *Salmonella* pathogenicity-associated island, SPI-1. SopE, along with SopE2, are guanine nucleotide exchange effector molecules for the type III secretion system encoded by SPI-1 (31). Together, these two molecules are able to act differentially on the RhoGTPase signaling cascade and may promote enhanced inflammatory function. SopE has also been shown to enhance murine colitis (32). SopE has previously been identified on a P2 family phage-like element in *S. Typhimurium* (33) and was associated with persistent epidemic strains in humans and animals. SopE has also been shown to reside on diverse phage types, including lambda-like phage in *Salmonella* Gallinarum, Enteritidis, Hadar, and Dublin (34), and was more common in the most common human serotypes in England (35). Therefore, the acquisition of SopE by contemporary and emergent subclade isolates may represent an advantage for their persistence and virulence.

Two gene disruptions were notable between the emergent and contemporary isolates of clade 1. First, emergent subclade isolates possessed a frameshift insertion of cytosine at position 680 in the *cirA* gene, resulting in a predicted frameshift that was uniform across emergent isolates. Additionally, a portion of the contemporary subclade isolates possessed a truncation of *cirA* that was independent of the mutation identified in emergent isolates. CirA is a catechol siderophore receptor that also serves as the receptor for colicin Collb, a pore-forming toxin produced by some *Escherichia coli* and *Salmonella* as a competitive exclusion mechanism (36). Collb production has been shown to favor producers during competition with Collb-sensitive strains lacking the plasmid that encodes this system (37). However, mutations in *cirA* have rendered Collb-sensitive strains resistant to the killing effects of Collb (38). Furthermore, Collb is commonly found to reside on IncI1 plasmids, which are ubiquitous among members of the family *Enterobacteriaceae* found in commercial turkeys (39, 40). Therefore, it is plausible that disruption of *cirA* in emergent subclade isolates provides a competitive advantage in the gastrointestinal tract against challenging Collb-positive bacteria. Because disruption of this gene was observed convergently in the contemporary and emergent subclades, it warrants further study.

A second gene disruption identified among emergent subclade isolates that was not present in contemporary or historical isolates was a deletion of a *uidA*-like sequence accompanied by deletion of an adjacent gene predicted to encode peptidoglycan deacetylase, PgdA. This region was intact in contemporary and historical isolates. Interestingly, clade 3 isolates were missing the entire *uidABC* region but retained *pgdA*. The presence of *uidABC* was sought among other phylogenetically proximal *Salmonella* serotypes (41) and was universally present, agreeing with previous studies identifying *Salmonella* clade-specific beta-glucuronidase activity (42). Together, this indicates that the *uidABC* system was ancestrally intact and subsequently truncated/deleted independently in clade 1 emergent and clade 3 isolates. The *uidABC* operon encodes enzymes capable of breaking down glucuronidated ligands, freeing them up as a bacterial nutrient source (43). This is typically viewed as a competitive advantage for gut

bacteria. However, because these systems were convergently inactivated in two distinct host-adapted clades of *S. Reading* and beta-glucuronidase systems are known to have a diverse array of functional effects in the gut (44), the possible role of inactivation of this system as a fitness benefit deserves further study.

This study was prompted by two large outbreaks of *S. Reading* in North America linked to the consumption of raw turkey products (23, 24). Our analyses indicate that these outbreaks coincide with the emergence of a novel successful clonal group of *S. Reading* in North America and dramatically increased rates of isolation of *S. Reading* in commercial turkey production, independent of company or geographical region. Given these facts, it is quite likely that the introduction of this clonal group occurred in commercial turkey production rapidly and uniformly. The most parsimonious explanation is that it was introduced vertically from a common source, likely through supply birds at the top of the genetic breeding pyramid. Interestingly, the emergence of this clonal group coincides with an outbreak of highly pathogenic avian influenza in 2015 that decimated turkey breeder supplies in the upper Midwestern United States (45). Thus, the emergence of this clonal group, combined with rapid repopulation efforts in the turkey industry, may have further contributed to its rapid spread. The microevolution of *S. Reading* in turkeys towards the emergent clade has apparently provided it with evolutionary advantages for success in the growing turkey, the turkey barn environment, and/or the human host. Limitations exist in this study, since it used retrospective samples from multiple sources with sometimes inconsistent methods of isolation and missing metadata. Therefore, while it is impossible at this time to pinpoint the precise source, this study highlights the power and utility of high-resolution genomics for better understanding the ecology and evolution of outbreaks of food-borne pathogens.

MATERIALS AND METHODS

Sample collection and DNA sequencing. Thirty-two isolates from this study were collected from commercial turkey production facilities in the United States between October 2016 and October 2018. Samples represent 32 unique premises within multiple turkey-producing companies. Samples were collected by boot sock sampling, environmental swabbing, fluff sampling, or cecal sampling. Enrichments were performed for *Salmonella* by primary enrichment of 1 g sample content in 9 ml in tetrathionate broth overnight with shaking at 42°C, followed by streaking of the primary enrichment onto XLD agar and incubation overnight at 37°C. Serotyping was performed on isolates following a standard protocol (46). DNA was extracted from cultures using the Qiagen DNeasy kit (Valencia, CA) following the manufacturer's instructions. Genomic DNA libraries were created using the Nextera XT library preparation kit and Nextera XT index kit v2 (Illumina, San Diego, CA), and sequencing was performed using 2x250-bp dual-index runs on an Illumina MiSeq at the University of Minnesota Mid-Central Research and Outreach Center (Willmar, MN).

Study population for phylogenomic analysis. A search of NCBI's Short Read Archive (SRA) was conducted for all available raw sequencing data of isolates annotated as *Salmonella enterica* subsp. *enterica* serotype Reading. Only isolates that met the following criteria were considered: (i) was collected within the United States, (ii) had a known isolation year, and (iii) had a known isolation source. Raw sequencing reads of all identified isolates ($n = 989$) were downloaded from the SRA using the SRA Toolkit (v2.8.2). The majority of animal and retail meat isolates were isolated as a part of U.S. Food Safety and Inspection Service (FSIS) monitoring and the U.S. Food and Drug Administration's National Antimicrobial Resistance Monitoring System (NARMS) programs. An additional 32 isolates collected from U.S. commercial turkey production facilities were sequenced for this study (see "Sample collection and DNA sequencing" above for details). A series of quality filtering steps within the bioinformatic processing pipeline (described below) were used to obtain a final sample size of 988 high-quality isolate genomes, including 566 from turkey-related sources (see Dataset S3A posted at <https://doi.org/10.6084/m9.figshare.11966550>). A summary of sample filtering steps is depicted in Fig. S11 posted at the above URL.

To investigate the two recent North American *S. Reading* outbreaks in the context of turkey-source *S. Reading* strains, raw sequencing reads from an additional 111 clinical *S. Reading* isolates collected by the Public Health Agency of Canada's (PHAC) National Microbiology Laboratory were downloaded from the SRA (see Dataset S3B at the above URL). U.S. and Canada clinical isolates were defined as part of the 2017 – 2019 outbreaks based on criteria that included analysis by whole-genome sequencing defined by the CDC and PHAC, respectively.

Genome assembly and quality assessment. All raw FASTQ files were trimmed and quality filtered using Trimmomatic (v0.33) (47), specifying removal of Illumina Nextera adapters, a sliding window of 4 with an average Phred quality score of 20, and 36 as the minimum read length. Trimmed reads were *de novo* assembled using the Shovill pipeline (v1.0.4), which utilizes the SPAdes assembler (48), with default parameters (<https://github.com/tseemann/shovill>). Assembly quality was assessed with QUAST (v5.0.0) (49). To calculate average sequencing depth of coverage, trimmed reads were mapped to assembled

contigs using the BWA-MEM algorithm (v0.7.17) (50), and a histogram of depth was computed using the *genomecov* command in BEDTools (v2.27.1) (51). Only isolates with an *N50* of $\geq 20,000$ bp and an average depth of $\geq 20\times$ were included in further analyses (see Fig. S11 posted at <https://doi.org/10.6084/m9.figshare.11966550>).

Serotype prediction. *In silico* serotype prediction was performed with the *Salmonella In Silico* Typing Resource (SISTR) (v1.0.2) (52). Only isolates with a predicted serotype of Reading for both antigen identification and cgMLST cluster analysis were included in downstream analyses (see Fig. S11 posted at the above URL).

Sequence typing. *In silico* multilocus sequence typing (MLST) was performed using the software, *mlst* (v2.16.1) (<https://github.com/tseemann/mlst>), with the Achtman seven-gene *Salmonella* MLST scheme hosted on the PubMLST website (<https://pubmlst.org>) (25). Core genome multilocus sequence typing (cgMLST) was performed on the Enterobase webserver using their custom *Salmonella* cgMLST V2 scheme of 3,002 loci (53). Because draft genomes of multiple contigs may frequently contain missing genes, cgMLST profiles were hierarchically clustered allowing for a mismatch of up to two or five alleles. Minimum spanning trees based on both the traditional MLST and cgMLST allelic profiles were generated in Enterobase's standalone software, GrapeTree (v1.5.0) (54).

Phylogenetic analysis. Single nucleotide polymorphisms (SNPs) were identified in each sample using Snippy (v4.4.0), with a minimum sequencing depth of $8\times$ (<https://github.com/tseemann/snippy>) and the *S. Reading* assembly, strain [SRR6374143](https://doi.org/10.6084/m9.figshare.11966550), as the reference. Separate core SNP alignments were then created for all isolates ($n = 988$) and for all clade 1 turkey-source isolates ($n = 565$). Based on MLST and cgMLST minimum spanning trees, one turkey isolate clustered separately from all other turkey isolates and was therefore not included in the turkey-source alignment. Recombinant regions were identified with Gubbins (v2.3.4) (55) and masked from the core genome alignments using maskrc-svg (v0.5) (<https://github.com/kwongj/maskrc-svg>). Samples with $>25\%$ missing data were removed from further analyses (see Fig. S11 posted at <https://doi.org/10.6084/m9.figshare.11966550>). The program *snp-sites* (v2.4.1) was then used to extract all core SNPs and monomorphic sites where the columns did not contain any gaps or ambiguous bases (56). Pairwise core SNP distance matrices were created using *snp-dists* (v0.6.3) (<https://github.com/tseemann/snp-dists>) after duplicate core SNP profiles were removed with SeqKit (v0.10.1) (57).

Maximum likelihood trees for both all isolates and the turkey-source-only isolates only were reconstructed based on the alignments of core SNPs plus monomorphic sites with IQ-TREE (v1.6.10) (58). ModelFinder was used to identify the most appropriate substitution models according to the Bayesian information criterion (59). For the "all-isolate" tree, the model with the best fit was the three substitution-type model (K3Pu) (60) with empirically derived unequal base frequencies (+F) and the discrete gamma model of rate heterogeneity model with four rate categories (+G4) (61). For the "turkey-source" tree, the best model was K3Pu+F+I, where the rate heterogeneity model (+I) allowed for a proportion of invariable sites. Branch support for both trees was estimated by performing 1,000 ultrafast bootstrap approximation replicates (see Fig. S3 posted at <https://doi.org/10.6084/m9.figshare.11966550>) (62). The resulting trees were visualized and annotated using the online tool iTOL (63).

To assess the robustness of clades identified in the turkey-source core SNP-based phylogenetic tree, two additional turkey-source trees were constructed using alternative methods based on the pan-genome (see "Pan-genome analyses" below for further details). First, a core genome phylogenetic tree was constructed from the core genome alignment. Core SNPs and monomorphic sites were then extracted from this alignment and used as input into ModelFinder and IQ-TREE. The best model was the transversion substitution model [AG = CT] (TVM) with empirically derived unequal base frequencies (+F) and allowing for a proportion of invariable sites (+I). Branch support was estimated from 1,000 ultrafast bootstrap approximation replicates. Second, a hierarchical clustering dendrogram was generated based on the presence/absence of pan-genome gene clusters. Euclidean distance was calculated using the R package, *vegan* (v2.5-5) (64), and complete linkage clustering was performed by the *hclust* function from the R package, *stats* (v3.6.1).

A separate maximum likelihood tree of all clade 1 turkey-source isolates ($n = 565$) and human-source isolates identified as part of the 2017 – 2019 *S. Reading* outbreaks in the United States ($n = 139$) and Canada ($n = 111$) was constructed following the same methods outlined above. As with the turkey-only tree, the best model was identified as K3Pu+F+I, with 1,000 ultrafast bootstrap approximation replicates to estimate branch support.

Time-scaled phylogenetic analysis. Nonduplicate turkey-origin isolates were used. A "temporal signal" of the data was evaluated by generating a linear regression of phylogenetic root-to-tip distances against the sampling dates using Tempest (v1.5) (65), and a positive correlation between root-to-tip distance and collection time ($R^2 = 0.46$) was demonstrated. In addition, the "temporal signal" was verified using a tip-date randomization test that was conducted using the package TipDatingBeast (v1.0.6) (66) in R (v3.4.3) (67). The evaluated TMRCA for the selected model (below) was compared between the real data and the randomized trials ($n = 20$), and no overlaps were found between the HPD₉₅ intervals and/or mean values (data not shown). A time-scaled phylogeny was constructed using BEAST (v 1.10.4) (68). A general time reversible (GTR) substitution model was used for nucleotide substitution and both "uncorrelated lognormal relaxed" and "strict" molecular clocks with different coalescent population models (i.e., constant growth, logistic growth, exponential growth, Gaussian Markov random field [GMRF] Bayesian skyride, and Bayesian skyline) were explored. In order to correct for ascertainment bias, the total number of each nucleotide in the reference genome (A, C, G, and T: 1,072,006, 1,166,842, 1,187,745, and 1,074,348, respectively) was manually incorporated in the xml files of all models. Log marginal likelihoods obtained using path sampling (PS)/stepping-stone sampling (SS) (69, 70) were compared. An evolution-

ary rate of 2.64×10^{-7} mutations per site per year, previously estimated for *S. l. 4*, [5], 12:ii– ST34 (E. Elnekave, S. L. Hong, S. Lim, D. Boxrud, A. Rovira, A. E. Mather, A. Perez, and J. Alvarez, unpublished data) was used as the mean estimation for the clock rate prior. Each model combination was tested for at least two independent Markov chain Monte Carlo (MCMC) runs of at least 200 million generations, with sampling every 20,000 generations. Convergence and proper mixing of all MCMC runs (effective sample size >200) and the agreement between two independent MCMC runs of the same model were verified manually in Tracer (v1.7.1) (71) after excluding 10% of the MCMC chain as a burn-in. The model with the highest log Bayes factor value was the GTR-uncorrelated lognormal relaxed-constant population growth combination. LogCombiner (v1.10.4) (68) was used to combine the two independent MCMC runs of the final model after exclusion of 10% burn-in period. The R package ggtree (v1.10.5) (72) was used for tree visualization.

Genetic feature identification. Acquired resistance genes and known chromosomal mutations conferring antibiotic resistance were identified in sample assemblies using staramr (v0.3.0) (<https://github.com/phac-nml/staramr>) with the ResFinder and PointFinder databases (73, 74). A minimum identity of 90% was used for matching to both databases, with default minimum coverage lengths of 60% for ResFinder and 95% for PointFinder. Plasmid replicon markers were identified using ABRicate (v.0.8.13) (<https://github.com/tseemann/abricate>) with the PlasmidFinder database (75) and a minimum identity of 90% and minimum coverage length of 60%. ABRicate was also used to screen sample assemblies for the two additional plasmid replicons, Col440II-like and ColRNAI-like (<https://github.com/StaPH-B/resistanceDetectionCDC>), as they were of interest, but not present in the PlasmidFinder database. A heatmap of the presence and absence of plasmid types and antimicrobial resistance genes was created with the R packages, ggtree (v1.16.4) and tidytree (v0.2.5) (72). To test for significant nonrandom associations between genomic features of interest, one-sided Fisher's exact tests were performed on 2×2 contingency tables using the R function, *fisher.test*, with the Benjamini-Hochberg (BH) procedure to adjust *P* values for multiple testing (76).

Plasmid and accessory element annotation and analysis. Based upon plasmid replicon results, two plasmids were selected belonging to IncQ1 and Col440II/RNAI-like replicons. These completed plasmids were searched via nucleotide BLAST across several isolates within each clade to confirm their conservation. Representative plasmid sequences were used from strain SRR8925563. Genes were predicted using Prokka (v1.13.4) (77), and plasmids were annotated and visualized via CLC Sequence Viewer (v8.0.0) (Qiagen, Aarhus, Denmark). For clade-to-clade chromosome comparisons, representative genome assemblies were retrieved for the historical subclade of clade 1 (SRR1583085), contemporary subclade of clade 1 (SRR2407706), emergent subclade of clade 1 (SRR6904571), and clade 3 (SRR5865228) and annotated via Prokka. MAUVE (78) was used to reorder chromosomal contigs of the draft assemblies to that of a completed *S. Reading* chromosome (GenBank accession no. CP030214) (79). MAUVE was then used to align representative chromosomes and compare for genomic differences.

Plasmid prevalence over time and serotypes. To determine the prevalence of the Col440II/ColRNAI-like plasmid in *Salmonella enterica* over time, a 282-bp region of the Col440II-like replicon was used to search the publicly available ENA and SRA databases (through December 2016; 90% identity threshold) (80). Metadata for sequences positive for the 282-bp target were downloaded from NCBI. Resistance gene content was determined using an in-house database adapted from ResFinder 3.0 (90% identity, 60% coverage cutoff). Sequenced isolates with both serotype and year of collection available were included in the analysis ($n = 100$).

Pan-genome analyses. Sample assemblies were annotated with Prokka, and a core genome alignment was generated using Roary (v3.12.0) (81). Coding sequences were clustered into "gene clusters" using the default 95% sequence identity. "Core genes" were defined as gene clusters identified in 100% of isolates, while an "accessory genes" were defined as clusters present in $<100\%$ of isolates. A presence/absence matrix heatmap of accessory genes was created using the *roary_plots.py* script (https://github.com/sanger-pathogens/Roary/tree/master/contrib/roary_plots). Scoary (v1.6.16) (82) was then used to conduct a pan-genome-wide association analysis comparing the prevalence of gene clusters between phylogenetic clades. Specifically, in the all-isolate trees, clade 1 isolates were compared to clade 3 isolates, and in the turkey-source tree, contemporary subclade isolates were compared separately to both emergent subclade and historical subclade isolates. Genes identically distributed across samples were collapsed into a single gene cluster with the *collapse* option. For the turkey-only tree, a gene cluster was reported as significantly associated with a particular subclade if it had a Benjamini-Hochberg (BH)-adjusted *P* value of ≤ 0.05 and was present in $\geq 60\%$ of isolates in one subclade and $\leq 40\%$ in the other subclade. The reference sequence(s) of each significant gene cluster were then annotated using the top hit(s) from a BLASTX search against the NCBI's nonredundant protein sequence database (80). Heatmaps comparing the percentage of genomes possessing the significant gene cluster between clades were created using the R package, ggplot2 (v3.2.0) (83). Because not all plasmid replicons of interest were identified by Prokka and thus were not included in the pan-genome analysis, separate 2×2 Fisher's exact tests were performed for each identified plasmid replicon with BH-adjusted *P* values. Follow-up annotations of bacteriophage regions in the *S. Reading* genome were conducted on a representative genome assembly from the contemporary subclade, SRR2407706, with the web-based phage search tool, PHASTER (84).

Data availability. Raw reads from isolates sequenced in this study are available at the NCBI Short Read Archive (SRA) under BioProject accession no. PRJNA601793. Supplemental data are available at <https://doi.org/10.6084/m9.figshare.11966550>.

ACKNOWLEDGMENTS

We thank the turkey producers of the United States for their willingness to collaborate in this study. Isolates and data for outbreak cases in Canada were provided courtesy of the PulseNet Canada Steering Committee and members of the Canadian Public Health Laboratory Network. Bioinformatics was supported using tools available from the Minnesota Supercomputing Institute. Sequencing reagents for this study were donated by the Mid-Central Research and Outreach Center, Willmar, MN, USA.

REFERENCES

- Foley SL, Johnson TJ, Ricke SC, Nayak R, Danzeisen J. 2013. *Salmonella* pathogenicity and host adaptation in chicken-associated serovars. *Microbiol Mol Biol Rev* 77:582–607. <https://doi.org/10.1128/MMBR.00015-13>.
- Foley SL, Lynne AM, Nayak R. 2008. *Salmonella* challenges: prevalence in swine and poultry and potential pathogenicity of such isolates. *J Anim Sci* 86:E149–E162. <https://doi.org/10.2527/jas.2007-0464>.
- Painter JA, Hoekstra RM, Ayers T, Tauxe RV, Braden CR, Angulo FJ, Griffin PM. 2013. Attribution of foodborne illnesses, hospitalizations, and deaths to food commodities by using outbreak data, United States, 1998–2008. *Emerg Infect Dis* 19:407–415. <https://doi.org/10.3201/eid1903.111866>.
- Interagency Food Safety Analytics Collaboration. 2018. Foodborne illness source attribution estimates for 2016 for *Salmonella*, *Escherichia coli* O157, *Listeria monocytogenes*, and *Campylobacter* using multi-year outbreak surveillance data, United States. Centers for Disease Control and Prevention, Atlanta, GA.
- Schutz H, Melb BS, Wurz MD. 1920. The paratyphoid B group. *Lancet* 1920:93–97.
- Mitrovic M. 1956. First report of paratyphoid infection in turkey poults due to *Salmonella reading*. *Poult Sci* 35:171–174. <https://doi.org/10.3382/ps.0350171>.
- Edwards PR, Bruner DW. 1943. The occurrence and distribution of salmonella types in the United States. *J Infect Dis* 72:58–67. <https://doi.org/10.1093/infdis/72.1.58>.
- Ekirri AB, MacKay RJ, Gaskin JM, Freeman DE, House AM, Giguere S, Troedsson MR, Schuman CD, von Chamier MM, Henry KM, Hernandez JA. 2009. Epidemiologic analysis of nosocomial *Salmonella* infections in hospitalized horses. *J Am Vet Med Assoc* 234:108–119. <https://doi.org/10.2460/javma.234.1.108>.
- Salehi TZ, Badouei MA, Madadgar O, Ghiasi SR, Tamai IA. 2013. Shepherd dogs as a common source for *Salmonella enterica* serovar Reading in Garmsar, Iran. *Turk J Vet Anim Sci* 37:102–105.
- Molla W, Molla B, Alemayehu D, Muckle A, Cole L, Wilkie E. 2006. Occurrence and antimicrobial resistance of *Salmonella* serovars in apparently healthy slaughtered sheep and goats of central Ethiopia. *Trop Anim Health Prod* 38:455–462. <https://doi.org/10.1007/s11250-006-4325-4>.
- Drachman RH, Petersen NJ, Boring JR, Payne FJ. 1958. Widespread *Salmonella* Reading infection of undetermined origin. *Public Health Rep* 73:885–894.
- Lienemann T, Niskanen T, Guedes S, Siitonen A, Kuusi M, Rimhanen-Finne R. 2011. Iceberg lettuce as suggested source of a nationwide outbreak caused by two *Salmonella* serotypes, Newport and Reading, in Finland in 2008. *J Food Prot* 74:1035–1040. <https://doi.org/10.4315/0362-028X.JFP-10-455>.
- Tanguay F, Vrbova L, Anderson M, Whitfield Y, Macdonald L, Tschetter L, Hexemer A, Salmonella Reading Investigation Team. 2017. Outbreak of *Salmonella* Reading in persons of Eastern Mediterranean origin in Canada, 2014–2015. *Can Commun Dis Rep* 43:14–20. <https://doi.org/10.14745/ccdr.v43i01a03>.
- Beli E, Telo A, Duraku E. 2001. *Salmonella* serotypes isolated from turkey meat in Albania. *Int J Food Microbiol* 63:165–167. [https://doi.org/10.1016/S0168-1605\(00\)00402-5](https://doi.org/10.1016/S0168-1605(00)00402-5).
- Hird DW, Kinde H, Case JT, Charlton BR, Chin RP, Walker RL. 1993. Serotypes of *Salmonella* isolated from California turkey flocks and their environment in 1984–89 and comparison with human isolates. *Avian Dis* 37:715–719. <https://doi.org/10.2307/1592019>.
- Poppe C, Kolar JJ, Demczuk WHB, Harris JE. 1995. Drug-resistance and biochemical characteristics of *Salmonella* from turkeys. *Can J Vet Res* 59:241–248.
- Centers for Disease Control and Prevention. 1991. Foodborne nosocomial outbreak of *Salmonella* Reading – Connecticut. *MMWR Morb Mortal Wkly Rep* 63:804–806.
- Dhakal J, Sharma CS, Nannapaneni R, McDaniel CD, Kim T, Kiess A. 2019. Effect of chlorine-induced sublethal oxidative stress on the biofilm-forming ability of *Salmonella* at different temperatures, nutrient conditions, and substrates. *J Food Prot* 82:78–92. <https://doi.org/10.4315/0362-028X.JFP-18-119>.
- Robertson LJ, Johannessen GS, Gjerde BK, Loncarevic S. 2002. Microbiological analysis of seed sprouts in Norway. *Int J Food Microbiol* 75:119–126. [https://doi.org/10.1016/S0168-1605\(01\)00738-3](https://doi.org/10.1016/S0168-1605(01)00738-3).
- Mollenkopf DF, Mathys DA, Dargatz DA, Erdman MM, Habing GG, Daniels JB, Wittum TE. 2017. Genotypic and epidemiologic characterization of extended-spectrum cephalosporin resistant *Salmonella enterica* from US beef feedlots. *Prev Vet Med* 146:143–149. <https://doi.org/10.1016/j.prevetmed.2017.08.006>.
- Ohta N, Norman KN, Norby B, Lawhon SD, Vinasco J, den Bakker H, Loneragan GH, Scott HM. 2017. Population dynamics of enteric *Salmonella* in response to antimicrobial use in beef feedlot cattle. *Sci Rep* 7:14310. <https://doi.org/10.1038/s41598-017-14751-9>.
- Blau DM, McCluskey BJ, Ladely SR, Dargatz DA, Fedorka-Cray PJ, Ferris KE, Headrick ML. 2005. *Salmonella* in dairy operations in the United States: prevalence and antimicrobial drug susceptibility. *J Food Prot* 68:696–702. <https://doi.org/10.4315/0362-028X-68.4.696>.
- Centers for Disease Control and Prevention. 2019. Outbreak of multidrug-resistant *Salmonella* infections linked to raw turkey products: final update. Centers for Disease Control and Prevention, Atlanta, GA. <https://www.cdc.gov/salmonella/reading-07-18/index.html>. Accessed October 2019.
- Public Health Agency of Canada. 2020. Public health notice — outbreak of *Salmonella* illnesses linked to raw turkey and raw chicken. <https://www.canada.ca/en/public-health/services/public-health-notices/2018/outbreak-salmonella-illnesses-raw-turkey-raw-chicken.html>. Accessed February 2020.
- Jolley KA, Bray JE, Maiden MCJ. 2018. Open-access bacterial population genomics: BIGSdb software, the PubMLST.org website and their applications. *Wellcome Open Res* 3:124. <https://doi.org/10.12688/wellcomeopenres.14826.1>.
- Klein JR, Fahlen TF, Jones BD. 2000. Transcriptional organization and function of invasion genes within *Salmonella enterica* serovar Typhimurium pathogenicity island 1, including the *prgH*, *prgl*, *prgJ*, *prgK*, *orgA*, *orgB*, and *orgC* genes. *Infect Immun* 68:3368–3376. <https://doi.org/10.1128/IAI.68.6.3368-3376.2000>.
- Centers for Disease Control and Prevention. 2011. Multistate outbreak of human *Salmonella* Hadar infections associated with turkey burgers. Centers for Disease Control and Prevention, Atlanta, GA.
- Centers for Disease Control and Prevention. 2012. Multistate outbreak of human *Salmonella* Hadar infections linked to live poultry in backyard flocks. Centers for Disease Control and Prevention, Atlanta, GA.
- Loftie-Eaton W, Rawlings DE. 2012. Diversity, biology and evolution of IncQ-family plasmids. *Plasmid* 67:15–34. <https://doi.org/10.1016/j.plasmid.2011.10.001>.
- Oliva M, Monno R, D'Addabbo P, Pesole G, Dionisi AM, Scarscia M, Chiara M, Horner DS, Manzari C, Luzzi I, Calia C, D'Erchia AM, Pazzani C. 2017. A novel group of IncQ1 plasmids conferring multidrug resistance. *Plasmid* 89:22–26. <https://doi.org/10.1016/j.plasmid.2016.11.005>.
- Friebe A, Ilchmann H, Aepfelbacher M, Ehrbar K, Machleidt W, Hardt WD. 2001. SopE and SopE2 from *Salmonella typhimurium* activate different sets of RhoGTPases of the host cell. *J Biol Chem* 276:34035–34040. <https://doi.org/10.1074/jbc.M100609200>.

32. Hapfelmeier S, Ehrbar K, Stecher B, Barthel M, Kremer M, Hardt WD. 2004. Role of the *Salmonella* pathogenicity island 1 effector proteins SipA, SopB, SopE, and SopE2 in *Salmonella enterica* subspecies 1 serovar Typhimurium colitis in streptomycin-pretreated mice. *Infect Immun* 72: 795–809. <https://doi.org/10.1128/IAI.72.2.795-809.2004>.
33. Mirolid S, Rabsch W, Rohde M, Stender S, Tschape H, Russmann H, Igwe E, Hardt WD. 1999. Isolation of a temperate bacteriophage encoding the type III effector protein SopE from an epidemic *Salmonella typhimurium* strain. *Proc Natl Acad Sci U S A* 96:9845–9850. <https://doi.org/10.1073/pnas.96.17.9845>.
34. Mirolid S, Rabsch W, Tschape H, Hardt WD. 2001. Transfer of the *Salmonella* type III effector sopE between unrelated phage families. *J Mol Biol* 312:7–16. <https://doi.org/10.1006/jmbi.2001.4950>.
35. Hopkins KL, Threlfall EJ. 2004. Frequency and polymorphism of *sopE* in isolates of *Salmonella enterica* belonging to the ten most prevalent serotypes in England and Wales. *J Med Microbiol* 53:539–543. <https://doi.org/10.1099/jmm.0.05510-0>.
36. Cascales E, Buchanan SK, Duche D, Kleanthous C, Lloubes R, Postle K, Riley M, Slatin S, Cavard D. 2007. Colicin biology. *Microbiol Mol Biol Rev* 71:158–229. <https://doi.org/10.1128/MMBR.00036-06>.
37. Stecher B, Denzler R, Maier L, Bernet F, Sanders MJ, Pickard DJ, Barthel M, Westendorf AM, Krogfelt KA, Walker AW, Ackermann M, Dobrindt U, Thomson NR, Hardt WD. 2012. Gut inflammation can boost horizontal gene transfer between pathogenic and commensal Enterobacteriaceae. *Proc Natl Acad Sci U S A* 109:1269–1274. <https://doi.org/10.1073/pnas.1113246109>.
38. Davies JK, Reeves P. 1975. Genetics of resistance to colicins in *Escherichia coli* K-12: cross-resistance among colicins of group B. *J Bacteriol* 123: 96–101. <https://doi.org/10.1128/JB.123.1.96-101.1975>.
39. Sanad YM, Johnson K, Park SH, Han J, Deck J, Foley SL, Kenney B, Ricke S, Nayak R. 2016. Molecular characterization of *Salmonella enterica* serovars isolated from a turkey production facility in the absence of selective antimicrobial pressure. *Foodborne Pathog Dis* 13:80–87. <https://doi.org/10.1089/fpd.2015.2002>.
40. Johnson TJ, Logue CM, Johnson JR, Kuskowski MA, Sherwood JS, Barnes HJ, DeRoy C, Wannemuehler YM, Obata-Yasuoka M, Spanjaard L, Nolan LK. 2012. Associations between multidrug resistance, plasmid content, and virulence potential among extraintestinal pathogenic and commensal *Escherichia coli* from humans and poultry. *Foodborne Pathog Dis* 9:37–46. <https://doi.org/10.1089/fpd.2011.0961>.
41. Laing CR, Whiteside MD, Gannon VPJ. 2017. Pan-genome analyses of the species *Salmonella enterica*, and identification of genomic markers predictive for species, subspecies, and serovar. *Front Microbiol* 8:1345. <https://doi.org/10.3389/fmicb.2017.01345>.
42. den Bakker HC, Moreno Switt AI, Govoni G, Cummings CA, Ranieri ML, Degoricija L, Hoelzer K, Rodriguez-Rivera LD, Brown S, Bolchacova E, Furtado MR, Wiedmann M. 2011. Genome sequencing reveals diversification of virulence factor content and possible host adaptation in distinct subpopulations of *Salmonella enterica*. *BMC Genomics* 12:425. <https://doi.org/10.1186/1471-2164-12-425>.
43. Liang WJ, Wilson KJ, Xie H, Knol J, Suzuki S, Rutherford NG, Henderson PJ, Jefferson RA. 2005. The *gusBC* genes of *Escherichia coli* encode a glucuronide transport system. *J Bacteriol* 187:2377–2385. <https://doi.org/10.1128/JB.187.7.2377-2385.2005>.
44. Dashnyam P, Mudududdla R, Hsieh TJ, Lin TC, Lin HY, Chen PY, Hsu CY, Lin CH. 2018. Beta-glucuronidases of opportunistic bacteria are the major contributors to xenobiotic-induced toxicity in the gut. *Sci Rep* 8:16372. <https://doi.org/10.1038/s41598-018-34678-z>.
45. Fitzpatrick A, Mor SK, Thurn M, Wiedenman E, Otterson T, Porter RE, Patnayak DP, Lauer DC, Voss S, Rossow S, Collins JE, Goyal SM. 2017. Outbreak of highly pathogenic avian influenza in Minnesota in 2015. *J Vet Diagn Invest* 29:169–175. <https://doi.org/10.1177/1040638716682058>.
46. Ewing WH. 1986. *Edward and Ewing's identification of Enterobacteriaceae*, 4th ed. Elsevier Science Publishing Co, Inc, New York, NY.
47. Bolger AM, Lohse M, Usadel B. 2014. Trimmomatic: a flexible trimmer for Illumina sequence data. *Bioinformatics* 30:2114–2120. <https://doi.org/10.1093/bioinformatics/btu170>.
48. Bankevich A, Nurk S, Antipov D, Gurevich AA, Dvorkin M, Kulikov AS, Lesin VM, Nikolenko SI, Pham S, Pribliski AD, Pyshkin AV, Sirotkin AV, Vyahhi N, Tesler G, Alekseyev MA, Pevzner PA. 2012. SPAdes: a new genome assembly algorithm and its applications to single-cell sequencing. *J Comput Biol* 19:455–477. <https://doi.org/10.1089/cmb.2012.0021>.
49. Gurevich A, Saveliev V, Vyahhi N, Tesler G. 2013. QUASt: quality assessment tool for genome assemblies. *Bioinformatics* 29:1072–1075. <https://doi.org/10.1093/bioinformatics/btt086>.
50. Li H, Durbin R. 2009. Fast and accurate short read alignment with Burrows-Wheeler transform. *Bioinformatics* 25:1754–1760. <https://doi.org/10.1093/bioinformatics/btp324>.
51. Quinlan AR, Hall IM. 2010. BEDTools: a flexible suite of utilities for comparing genomic features. *Bioinformatics* 26:841–842. <https://doi.org/10.1093/bioinformatics/btq033>.
52. Yoshida CE, Kruczkiewicz P, Laing CR, Lingohr EJ, Gannon VP, Nash JH, Taboada EN. 2016. The *Salmonella* In Silico Typing Resource (SISTR): an open web-accessible tool for rapidly typing and subtyping draft *Salmonella* genome assemblies. *PLoS One* 11:e0147101. <https://doi.org/10.1371/journal.pone.0147101>.
53. Alikhan NF, Zhou Z, Sergeant MJ, Achtman M. 2018. A genomic overview of the population structure of *Salmonella*. *PLoS Genet* 14:e1007261. <https://doi.org/10.1371/journal.pgen.1007261>.
54. Zhou Z, Alikhan NF, Sergeant MJ, Luhmann N, Vaz C, Francisco AP, Carrico JA, Achtman M. 2018. GrapeTree: visualization of core genomic relationships among 100,000 bacterial pathogens. *Genome Res* 28: 1395–1404. <https://doi.org/10.1101/gr.232397.117>.
55. Croucher NJ, Page AJ, Connor TR, Delaney AJ, Keane JA, Bentley SD, Parkhill J, Harris SR. 2015. Rapid phylogenetic analysis of large samples of recombinant bacterial whole genome sequences using Gubbins. *Nucleic Acids Res* 43:e15. <https://doi.org/10.1093/nar/gku1196>.
56. Page AJ, Taylor B, Delaney AJ, Soares J, Seemann T, Keane JA, Harris SR. 2016. SNP-sites: rapid efficient extraction of SNPs from multi-FASTA alignments. *Microb Genom* 2:e000056. <https://doi.org/10.1099/mgen.0.000056>.
57. Shen W, Le S, Li Y, Hu FQ. 2016. SeqKit: a cross-platform and ultrafast toolkit for FASTA/Q file manipulation. *PLoS One* 11:e0163962. <https://doi.org/10.1371/journal.pone.0163962>.
58. Nguyen LT, Schmidt HA, von Haeseler A, Minh BQ. 2015. IQ-TREE: a fast and effective stochastic algorithm for estimating maximum-likelihood phylogenies. *Mol Biol Evol* 32:268–274. <https://doi.org/10.1093/molbev/msu300>.
59. Kalyaanamoorthy S, Minh BQ, Wong TKF, von Haeseler A, Jermini LS. 2017. ModelFinder: fast model selection for accurate phylogenetic estimates. *Nat Methods* 14:587–589. <https://doi.org/10.1038/nmeth.4285>.
60. Takahata N, Kimura M. 1981. A model of evolutionary base substitutions and its application with special reference to rapid change of pseudogenes. *Genetics* 98:641–657.
61. Yang Z. 1994. Maximum likelihood phylogenetic estimation from DNA sequences with variable rates over sites: approximate methods. *J Mol Evol* 39:306–314. <https://doi.org/10.1007/BF00160154>.
62. Hoang DT, Chernomor O, von Haeseler A, Minh BQ, Vinh LS. 2018. UFBoot2: improving the ultrafast bootstrap approximation. *Mol Biol Evol* 35:518–522. <https://doi.org/10.1093/molbev/msx281>.
63. Letunic I, Bork P. 2019. Interactive Tree Of Life (iTOL) v4: recent updates and new developments. *Nucleic Acids Res* 47:W256–W259. <https://doi.org/10.1093/nar/gkz239>.
64. Oksanen J, Blanchet FG, Kindt R, Legendre P, Minchin PR, O'Hara RB, Simpson GL, Solymos P, Stevens MH, Wagner H. 2013. vegan: community ecology package, R package version 2.0-10. <http://CRAN.R-project.org/package=vegan>.
65. Rambaut A, Lam TT, Max Carvalho L, Pybus OG. 2016. Exploring the temporal structure of heterochronous sequences using TempEst (formerly Path-O-Gen). *Virus Evol* 2:vev007. <https://doi.org/10.1093/ve/vev007>.
66. Rieux A, Khatchikian CE. 2017. tipdatingbeast: an R package to assist the implementation of phylogenetic tip-dating tests using beast. *Mol Ecol Resour* 17:608–613. <https://doi.org/10.1111/1755-0998.12603>.
67. R Core Team. 2016. R: a language and environment for statistical computing. R Foundation for Statistical Computing, Vienna, Austria. <https://www.R-project.org/>.
68. Suchard MA, Lemey P, Baele G, Ayres DL, Drummond AJ, Rambaut A. 2018. Bayesian phylogenetic and phylodynamic data integration using BEAST 1.10. *Virus Evol* 4:vey016. <https://doi.org/10.1093/ve/vey016>.
69. Baele G, Lemey P, Bedford T, Rambaut A, Suchard MA, Alekseyenko AV. 2012. Improving the accuracy of demographic and molecular clock model comparison while accommodating phylogenetic uncertainty. *Mol Biol Evol* 29:2157–2167. <https://doi.org/10.1093/molbev/mss084>.
70. Baele G, Li WL, Drummond AJ, Suchard MA, Lemey P. 2013. Accurate model selection of relaxed molecular clocks in Bayesian phylogenetics. *Mol Biol Evol* 30:239–243.

71. Rambaut A, Drummond AJ, Xie D, Baele G, Suchard MA. 2018. Posterior summarization in Bayesian phylogenetics using Tracer 1.7. *Syst Biol* 67:901–904. <https://doi.org/10.1093/sysbio/syy032>.
72. Yu G, Smith DK, Zhu H, Guan Y, Lam TTY. 2017. ggtree: an R package for visualization and annotation of phylogenetic trees with their covariates and other associated data. *Methods Ecol Evol* 8:28–36. <https://doi.org/10.1111/2041-210X.12628>.
73. Zankari E, Hasman H, Cosentino S, Vestergaard M, Rasmussen S, Lund O, Aarestrup FM, Larsen MV. 2012. Identification of acquired antimicrobial resistance genes. *J Antimicrob Chemother* 67:2640–2644. <https://doi.org/10.1093/jac/dks261>.
74. Zankari E, Allesoe R, Joensen KG, Cavaco LM, Lund O, Aarestrup FM. 2017. PointFinder: a novel web tool for WGS-based detection of antimicrobial resistance associated with chromosomal point mutations in bacterial pathogens. *J Antimicrob Chemother* 72:2764–2768. <https://doi.org/10.1093/jac/dkx217>.
75. Carattoli A, Zankari E, Garcia-Fernandez A, Voldby Larsen M, Lund O, Villa L, Moller Aarestrup F, Hasman H. 2014. In silico detection and typing of plasmids using PlasmidFinder and plasmid multilocus sequence typing. *Antimicrob Agents Chemother* 58:3895–3903. <https://doi.org/10.1128/AAC.02412-14>.
76. Benjamini Y, Hochberg Y. 1995. Controlling the false discovery rate: a practical and powerful approach to multiple testing. *J R Statist Soc* 57:289–300.
77. Seemann T. 2014. Prokka: rapid prokaryotic genome annotation. *Bioinformatics* 30:2068–2069. <https://doi.org/10.1093/bioinformatics/btu153>.
78. Darling AC, Mau B, Blattner FR, Perna NT. 2004. Mauve: multiple alignment of conserved genomic sequence with rearrangements. *Genome Res* 14:1394–1403. <https://doi.org/10.1101/gr.2289704>.
79. Bessonov K, Robertson JA, Lin JT, Liu K, Gurnik S, Kernaghan SA, Yoshida C, Nash JHE. 2018. Complete genome and plasmid sequences of 32 *Salmonella enterica* strains from 30 serovars. *Microbiol Resour Announc* 7:e01232-18.
80. Bradley P, den Bakker HC, Rocha EPC, McVean G, Iqbal Z. 2019. Ultrafast search of all deposited bacterial and viral genomic data. *Nat Biotechnol* 37:152–159. <https://doi.org/10.1038/s41587-018-0010-1>.
81. Page AJ, Cummins CA, Hunt M, Wong VK, Reuter S, Holden MT, Fookes M, Falush D, Keane JA, Parkhill J. 2015. Roary: rapid large-scale prokaryote pan genome analysis. *Bioinformatics* 31:3691–3693. <https://doi.org/10.1093/bioinformatics/btv421>.
82. Brynildsrud O, Bohlin J, Scheffer L, Eldholm V. 2016. Rapid scoring of genes in microbial pan-genome-wide association studies with Scoary. *Genome Biol* 17:238. <https://doi.org/10.1186/s13059-016-1108-8>.
83. Wickham H. 2016. ggplot2: elegant graphics for data analysis. Springer-Verlag, New York, NY.
84. Arndt D, Grant JR, Marcu A, Sajed T, Pon A, Liang Y, Wishart DS. 2016. PHASTER: a better, faster version of the PHAST phage search tool. *Nucleic Acids Res* 44:W16–W21. <https://doi.org/10.1093/nar/gkw387>.